Dynamics Modelling of Hexaslides using the Decoupled Natural Orthogonal Complement Matrices

A. B. KOTESWARA RAO[1] S. K. SAHA[2,*] and P. V. M. RAO[2]
[1]*Mechanical Engineering Department, G.V.P. College of Engg, Visakhapatnam-530041, India*
[2]*Mechanical Engineering Department, I.I.T. Delhi, Hauz Khas, New Delhi-110016, India; E-mail: saha@mech.iitd.ernet.in.*

Abstract. In this paper, dynamic model of a class of parallel systems, namely, the hexaslides, is proposed. The model developed is based on the concept the decoupled natural orthogonal complement (DeNOC) matrices, introduced elsewhere. The dynamic model of hexslides, though complex due to the existence of multi-loop kinematic chains, is required for actuator power estimation, computed-torque control, optimum tool trajectory generation, etc. The use of DeNOC offers many physical interpretations, recursive algorithms, and parallel computations. Using the proposed dynamic model, a parallel inverse dynamics algorithm has been presented to compute the actuator forces. This is useful to choose suitable motors for an application. An illustration is provided using an existing machine tool based on hexaslides, namely, the HexaM, while it is carrying out a circular contouring. Secondly, the effect of leg and slider inertias is also studied, which clearly suggests that neither of these can be neglected while finding the actuator forces.

Keywords: Hexaslides, Parallel architecture, Dynamics modelling, DeNOC matrices

1. Introduction

The parallel kinematic machines (PKMs) offering six degree of freedom (DOF) can be broadly classified as (i) Hexapods [1, 2] having variable-length struts and (ii) Hexaslides [3–5] having fixed-length legs, as shown in Figure 1. In case of Hexapods, the variation in leg-lengths determines the position and orientation of the moving tool platform or the end effector in the 3-dimensional Cartesian space. On the other hand, the movement of the sliders connecting the fixed platform and the legs decide the position and orientation of the tool platform of Hexaslides. Actuators, usually the heavy parts of the hexaslides, are fixed at the base so that the machine carries only the lighter masses, i.e., the legs, joint assemblies, and the moving platform. Hence, higher velocities and accelerations are achievable at the end-effector of the hexaslides. The three major machine tools based on Hexaslide architecture are (i) Hexaglide with coplanar-parallel rails [3]; (ii) HexaM with slanted rails [4]; and (iii) Linapod with vertical rails [5]. A general hexaslide
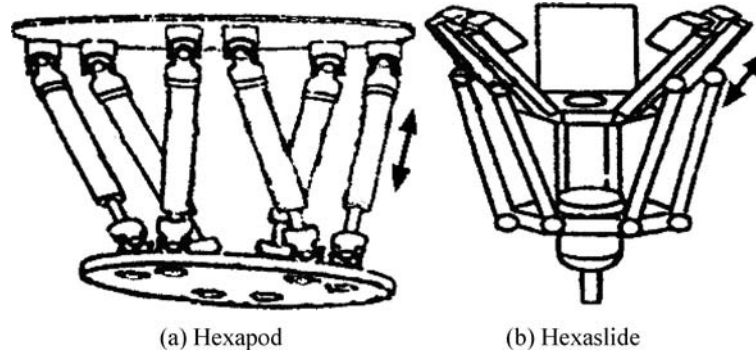
(a) Hexapod   (b) Hexaslide

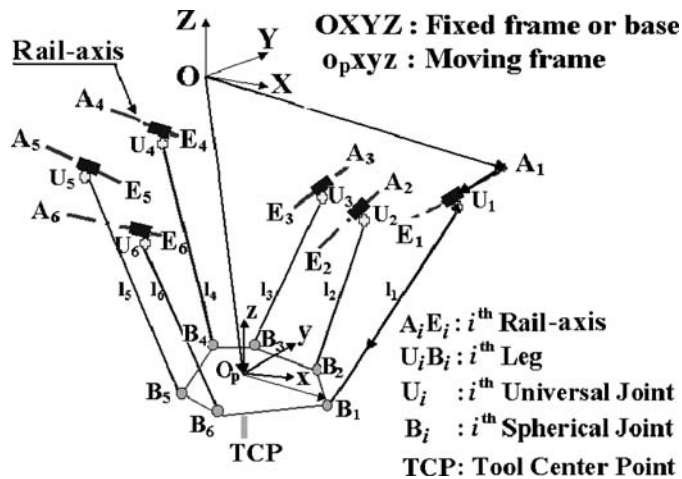*Figure 1*. Parallel kinematic machines.

Figure 2. A general hexaslide machine tool.

machine tool is shown in Figure 2. The sliders move along the six distinct rail-axes, A_iE_i, whereas the legs of constant length are connected to the sliders through universal joints, U_i. Other end of each leg is connected to the tool platform through spherical joints, B_i.

The kinematics of parallel manipulators has been studied extensively, whereas fewer papers can be found on dynamics [6–8]. Formulation methods to derive the dynamics equations of motion of a mechanical system fall mainly into two categories, namely, (i) Euler-Lagrange (EL), and (ii) Newton-Euler (NE) [8]. Unlike in serial kinematic chain mechanical systems, in multi-loop mechanical systems like in hexaslides all the joint variables are not independent due to the existence of non-linear loop closure constraints. The closed-loops of the system make the dynamic computations more complex and computationally expensive. The computational recursiveness of many methods [9] and others applicable to serial manipulators

is far from being straightforward when applied to PKMs. Several algorithms of inverse dynamics of PKMs, [9–13] and others, were reported in the past few years. Adopting the NE approach, Kim and Ryu [14, 15] developed the forward and inverse dynamics equations of hexaslides.

In order to take the advantages of the efficient algorithms of the serial chain manipulators for the analysis of PKMs, the common methods to deal with their closed-loops are: (i) to cut the loops, introduce Lagrange multipliers to substitute for the cut joints, and apply the recursive scheme for the cut loops [16], and others; (ii) to use the close-loop constraints to relate the unactuated joint rates in terms of the actuated joint rates, and obtain a set of independent dynamics equations of motion [17]. The concept of an orthogonal complement, namely, the *Natural Orthogonal Complement* (NOC) was introduced in [18]. The NOC is defined as the linear transformation that maps the independent joint velocities into the generalized twist of the system. The matrix is an orthogonal complement of the *velocity constraint matrix* [18] arising out of the joints present in the system. The dynamic modeling based on the NOC was found advantageous in [19, 20] and others. The derivation of the NOC for closed-loop systems is tedious because the explicit expressions of the loop-constraint equations and the associated Jacobian matrices must be derived. To avoid the abovementioned difficulty, a numerical method, proposed in [21], was used in [22], and others. Recently, Xi and Sinatra [23] reported the inverse dynamics of hexapods with fixed length legs using the NOC matrix.

On the other hand, Saha [24] expressed the NOC, explicitly, as a product of two matrices, namely, a block lower triangular and a block diagonal. Some of the advantages due to this approach are: (i) Many physical interpretations of the vectors and matrices, e.g., twist-propagation matrix, etc.; (ii) Recursive inverse and forward dynamics algorithms, and others. Saha and Schiehlen [25] showed that the NOC of a closed-loop parallel manipulator can be split into three matrices, namely, the lower-block triangular, the full-block, and the block-diagonal. Later, however, Khan [26] used the concept of the DeNOC for the closed-loop systems to show that the methodology can be suitably adopted for parallel computations in multi-platform computers. In the present work, the dynamic model of hexaslides based on the DeNOC matrices, which facilitates parallel computations, is developed. Unlike in Xi and Sinatra [23], the masses and inertias of all moving bodies including the sliders are considered in the proposed model.

This paper is organized as follows: Section 2 presents the kinematic analysis of hexaslides required for the dynamic modeling, as given in Section 3. A parallel inverse dynamics algorithm is proposed in Section 4. The use of the proposed algorithm is illustrated with an existing machine tool based on hexaslides, namely, the HexaM [4, 15, 27], while carrying out a circular contouring in Section 5. Effect of the inertia of different bodies is presented in Section 6. Finally, the conclusions are given in Section 7.
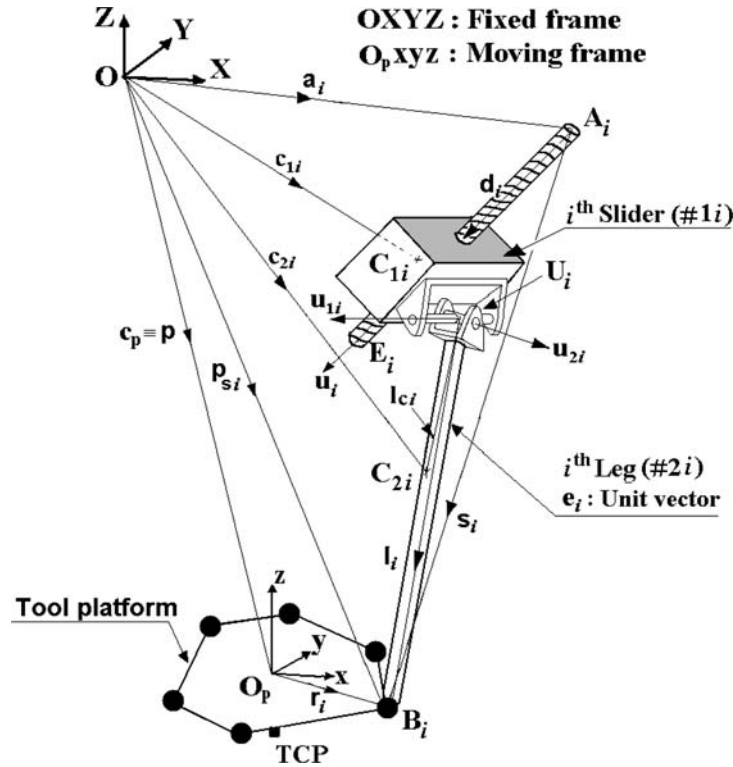
Figure 3. The ith kinematic chain of a hexslide.

2. Knematic Analysis

In this section, kinematic analysis, i.e., the relations between the positions and velocities of varies bodies, namely, the sliders and tool platform, of a hexaslide are derived. Using the loop mobility criteria [6], the DOF of a general hexaslide can be obtained as six. First, the following notations are introduced: Referring to Figure 3

O-XYZ: Fixed frame of reference attached to the base;

O_p-xyz: Moving frame attached to the tool platform;

O_P: mass centre of the end-effector, i.e., the tool platform; **R**: The 3×3 Rotation matrix representing the orientation of the moving frame, O_p-xyz, with rerespect to the fixed frame, O-XYZ.

$\mathbf{p} \equiv \overline{OO_P} \equiv [p_x, p_y, p_z]^T$: The position of the mass center of the moving platform in the fixed frame, where p_x, p_y and p_z are the three Cartesian coordinates of the the point O_P; and for $i = 1, 2, \ldots, 6$

$L_i \equiv U_i B_i$: Length of the ith leg;

$S_i \equiv A_i E_i$: Length of the ith rail or stroke length of the ith actuator;

d_i : Distance of the ith slider from the starting point of ith rail;

u_i: Unit vector along the ith rail-axis;

$\mathbf{e}_i$: Unit vector along the ith leg;

$\mathbf{a}_i \equiv \overline{OA_i}$: Position vector of A_i with respect to the origin of the fixed frame;

$\mathbf{d}_i \equiv \overline{A_i U_i} = d_i \mathbf{u}_i$: Position vector of U_i with respect to point A_i;

$\mathbf{l}_i \equiv \overline{U_i B_i} = L_i \mathbf{e}_i$: Vector denoting the length of the ith leg;

$\mathbf{s}_i \equiv \overline{A_i B_i}$: Position vector of the center of the ith spherical joint on the tool platform;

$\mathbf{p}_{s_i} \equiv \overline{OB_i}$: Position vector of B_i with respect to the origin of the fixed frame;

$\mathbf{r'}_i \equiv \overline{O_P B_i}$: Position vector of B_i with respect to the reference point, i.e., point O_P, represented in the moving frame;

$\mathbf{r}_i \equiv \overline{O_P B_i}$: Position vector of B_i with respect to the reference point, i.e., point O_P, represented in the fixed frame;

C_{1_i} and C_{2_i}: mass centres of the 1st and 2nd links of the ith chain, i.e., slider and leg, respectively;

$\mathbf{c}_P$, $\mathbf{v}_P$, and $\dot{\mathbf{v}}_P$: 3-dimensional position, velocity and acceleration vectors of the mass centre, O_P, respectively;

$\mathbf{c}_{1_i}$ and $\mathbf{c}_{2_i}$: 3-dimensional position vectors of mass centres, C_{1_i} and C_{2_i}, respectively;

$\mathbf{v}_{1i}$ and $\mathbf{v}_{2i}$: 3-dimensional velocity vectors of mass centres, C_{1_i} and C_{2_i}, respectively;

$\dot{\mathbf{v}}_{1i}$ and $\dot{\mathbf{v}}_{2i}$: 3-dimensional acceleration vectors of mass centres, C_{1_i} and C_{2_i}, respectively;

ω_P and $\dot{\omega}_P$: 3-dimensional angular velocity and acceleration vectors of the tool platform;

ω_{1i} and ω_{2i}: 3-dimensional angular velocity vectors of 1st and 2nd links of the ith chain, respectively;

$\dot{\omega}_{1i}$ and $\dot{\omega}_{2i}$: 3-dimensional angular acceleration vectors of 1st and 2nd links of the ith chain, respectively.

However, $\omega_{1i} = \dot{\omega}_{1i} = \mathbf{0}$, since the 1st link of any chain, i.e., slider, has only translation.

2.1. POSITION ANALYSIS

Considering the loop, $O\,A_i\,U_i\,B_i\,O_p\,O$, Figure 3, the vector $\mathbf{s}_i$, for $i = 1, 2, \ldots, 6$, is written as,

$$\mathbf{s}_i \equiv \mathbf{p} + \mathbf{R}\mathbf{r}'_i - \mathbf{a}_i = \mathbf{d}_i + \mathbf{l}_i \tag{1}$$

Noting that, $\mathbf{r}_i = \mathbf{R}\mathbf{r}'_i$, and $\mathbf{d}_i \equiv d_i \mathbf{u}_i$, and $\mathbf{l}_i \equiv L_i \mathbf{e}_i$, Equation (1) can be rewritten as

$$\mathbf{s}_i - d_i \mathbf{u}_i = L_i \mathbf{e}_i \tag{2}$$

Performing the dot products of the left and right hand vectors of (2), one obtains

$$\left(\mathbf{s}_i - d_i \mathbf{u}_i\right)^{\mathrm{T}} \left(\mathbf{s}_i - d_i \mathbf{u}_i\right) = \mathrm{L}_i^2 \tag{3}$$

where $\mathbf{e}_i^{\mathrm{T}} \mathbf{e}_i = 1$ is used. Solution of (3) gives an explicit expression for d_i as

$$d_i = \left(\mathbf{s}_i^{\mathrm{T}} \mathbf{u}_i\right) \pm \sqrt{\left(\mathbf{s}_i^{\mathrm{T}} \mathbf{u}_i\right)^2 - \left(\mathbf{s}_i^{\mathrm{T}} \mathbf{s}_i - \mathrm{L}_i^2\right)}, \quad \text{for} \quad i = 1, 2, \ldots, 6 \tag{4}$$

Using (4), the *inverse kinematics problem*, i.e., to find the position of the actuators on their respective rails, d_i, for a given pose of the tool platform, i.e., $\mathbf{p}$ and $\mathbf{R}$, can be solved. Note that, (4) offers two values of d_i, say, $d_i^{(1)}$ and $d_i^{(2)}$. The given pose of the tool platform is said to be achievable if the values of d_i satisfy the constraint:

$$0 \leq d_i \leq S_i \quad \text{for } i = 1, 2, \ldots, 6 \tag{5}$$

and the constraints due to the allowed motion range of the universal and spherical joints.

2.2. VELOCITY ANALYSIS

The relations between the velocities of the tool platform and the actuators of a hexaslide are derived. Differentiation of (1) with respect to time yields

$$\dot{\mathbf{s}}_i = \dot{\mathbf{p}} + \dot{\mathbf{R}} \mathbf{r}_i' + \mathbf{R} \dot{\mathbf{r}}_i' - \dot{\mathbf{a}}_i = \dot{\mathbf{d}}_i + \dot{\mathbf{l}}_i \tag{6}$$

Noting, $\dot{\mathbf{p}} \equiv \mathbf{v}_{\mathrm{p}}$, $\dot{\mathbf{r}}_i' = \mathbf{0}$, $\dot{\mathbf{R}} \mathbf{r}_i' = \omega_{\mathrm{p}} \times \mathbf{R} \mathbf{r}_i'$, $\dot{\mathbf{a}}_i = \mathbf{0}$, $\dot{\mathbf{d}}_{i_i} = \dot{d}_i \mathbf{u}_i$, and $\dot{\mathbf{l}}_i = \omega_{2i} \times \mathbf{l}_i$, wherein $\dot{d}_i$ is the linear speed of the ith actuator, the above equation, (6), is rewritten as

$$\dot{d}_i \mathbf{u}_i = \mathbf{v}_{\mathrm{p}} + \omega_{\mathrm{p}} \times \mathbf{r}_i - \omega_{2i} \times \mathbf{l}_i \tag{7}$$

Taking the dot product of $\mathbf{e}_i$ on both sides of (7) yields

$$\dot{d}_i \mathbf{l}_i^{\mathrm{T}} \mathbf{u}_i = \mathbf{l}_i^{\mathrm{T}} \left[\mathbf{v}_{\mathrm{p}} + \omega_{\mathrm{p}} \times \mathbf{r}_i\right] \tag{8}$$

where $\mathbf{l}_i^{\mathrm{T}} (\omega_{2i} \times \mathbf{l}_i) = 0$ is used. Combining (8), for $i = 1, 2, \ldots, 6$, in a matrix form yields

$$\mathbf{J}_{\mathrm{a}} \dot{\mathbf{d}} = \mathbf{J}_{\mathrm{t}} \mathbf{t}_{\mathrm{P}} \tag{9}$$

where $\mathbf{t}_P \equiv \left[\, \omega_p^T \; \mathbf{v}_p^T \,\right]^T$: the 6-dimensional vector of the end-effector twist; $\dot{\mathbf{d}} \equiv \left[\, \dot{d}_1 \cdots \dot{d}_6 \,\right]^T$: the 6-dimensional vector of actuator rates; and the 6×6 matrices, $\mathbf{J}_a$ and $\mathbf{J}_t$, are given by

$$\mathbf{J}_a \equiv \begin{bmatrix} \mathbf{e}_1^T \mathbf{u}_1 & & & \\ & \cdot & & \\ & & \cdot & \\ & & & \cdot \\ & & & \mathbf{e}_6^T \mathbf{u}_6 \end{bmatrix}; \;\; \text{and} \;\; \mathbf{J}_t \equiv \begin{bmatrix} (\mathbf{r}_1 \times \mathbf{e}_1)^T & \mathbf{e}_1^T \\ \cdot & \cdot \\ \cdot & \cdot \\ \cdot & \cdot \\ (\mathbf{r}_6 \times \mathbf{e}_6)^T & \mathbf{e}_6^T \end{bmatrix} \tag{10}$$

Equation (9) can be rewritten as

$$\dot{\mathbf{d}} = \mathbf{J}\mathbf{t}_P, \text{ where } \mathbf{J} \equiv \mathbf{J}_a^{-1}\mathbf{J}_t \tag{11}$$

where the 6×6 matrix, $\mathbf{J}$, is known as the velocity Jacobian matrix of the tool platform. Now, referring to Figure 3, the following can be written:

$$\mathbf{c}_P = \mathbf{p}; \qquad \mathbf{c}_{1_i} = \mathbf{a}_i + d_i\mathbf{u}_i; \qquad \mathbf{c}_{2_i} = \mathbf{c}_{1_i} + \mathbf{l}_{ci} \tag{12a}$$

where $\mathbf{l}_{ci}$ is the 3-dimensional vector of mass centre of ith leg. Time derivative of (12a)

$$\mathbf{v}_P = \dot{\mathbf{c}}_P = \dot{\mathbf{p}}; \qquad \mathbf{v}_{1i} = \dot{d}_i\mathbf{u}_i; \qquad \mathbf{v}_{2i} = \mathbf{v}_{1i} + \omega_{2i} \times \mathbf{l}_{ci} \tag{12b}$$

where $\dot{\mathbf{u}}_i = \mathbf{0}$ is used. Time derivative of (12b) yields

$$\dot{\mathbf{v}}_P = \ddot{\mathbf{c}}_P = \ddot{\mathbf{p}}; \quad \dot{\mathbf{v}}_{1i} = \ddot{d}_i\mathbf{u}_i; \quad \dot{\mathbf{v}}_{2i} = \dot{\mathbf{v}}_{1i} + (\dot{\omega}_{2i} \times \mathbf{l}_{ci}) + \omega_{2i} \times (\omega_{2i} \times \mathbf{l}_{ci}) \tag{12c}$$

2.2.1. *Angular velocity of legs*

In this section, angular velocity of legs, ω_{2i}, is derived. Equation (7) is expressed as

$$\Lambda_{li}\omega_{2i} = \frac{-1}{L_i}[\mathbf{v}_p - \Lambda_{ri}\omega_p - \dot{d}_i\mathbf{u}_i] \tag{13}$$

where the 3×3 skew-symmetric matrices, namely, Λ_{li} and Λ_{ri}, are the cross-product matrices associated with vectors $\mathbf{e}_i$ and $\mathbf{r}_i$, respectively. A cross-product matrix, $\mathbf{X}$, associated with the vector, $\mathbf{x}$, is defined as, $\mathbf{X} \equiv \mathbf{x} \times \mathbf{1}$, such that, $\mathbf{X}\mathbf{a} \equiv \mathbf{x} \times \mathbf{a}$, for any arbitrary vector $\mathbf{a}$, and $\mathbf{1}$ being the 3×3 identity matrix. In order to find ω_{2i}, (13) alone cannot be used since Λ_{li} is always singular. The universal joint, U_i, constrains the orientation of each leg allowing only 2-DOF rotation. This can be expressed as

$$(\mathbf{u}_{1i} \times \mathbf{u}_{2i})^T\omega_{2i} = 0 \tag{14}$$

for $i = 1, 2, \ldots, 6$. Vectors $\mathbf{u}_{1i}$ and $\mathbf{u}_{2i}$ are the unit vectors along the 1st and 2nd axes of the ith universal joint, respectively. Equation (14) signifies that the component of the angular velocity of the ith leg along the axis orthogonal to $\mathbf{u}_{1i}$ and $\mathbf{u}_{2i}$ vanishes. For the universal joints, $\mathbf{u}_{1i}$ is assumed to be attached to the ith rail, and hence, is independent of pose of the tool platform. The vector $\mathbf{u}_{2i}$ is configuration dependent, and is expressed as

$$\mathbf{u}_{2i} = \mathbf{u}_{1i} \times \mathbf{e}_i \tag{15}$$

Substitution of (15) in (14) and simpification yields

$$\left(\Lambda_{ui}^2 \mathbf{e}_i\right)^{\mathrm{T}} \omega_{2i} = 0 \tag{16}$$

where Λ_{ui} is the 3×3 cross-product matrix associated with vector $\mathbf{u}_{1i}$, as defined after (13), and $\Lambda_{ui}^2 \equiv \Lambda_{ui}\Lambda_{ui} = \mathbf{u}_{1i}\mathbf{u}_{1i}^{\mathrm{T}} - \mathbf{1}$, for $i = 1, 2, \ldots, 6$. Combining (13) and (16), one gets

$$\bar{\mathbf{A}}_i \omega_{2i} = \Delta_i \tag{17a}$$

wherein the 4×3 matrix, $\bar{\mathbf{A}}_i$, and the 4-dimensional vector, Δ_i, are as follows:

$$\bar{\mathbf{A}}_i \equiv \begin{bmatrix} \Lambda_{li} \\ (\Lambda_{ui}^2 \mathbf{e}_i)^{\mathrm{T}} \end{bmatrix} \text{ and } \Delta_i \equiv \frac{-1}{L_i} \begin{bmatrix} \mathbf{v}_{\mathrm{p}} - \Lambda_{ri}\omega_{\mathrm{p}} - \dot{\mathrm{d}}_i \mathbf{u}_i \\ 0 \end{bmatrix} \tag{17b}$$

Using the definition of Moore-Penrose generalized inverse for the overdetermined system of equations [28], the angular velocity of the ith leg, ω_{2i}, can be found from (17a) as

$$\omega_{2i} = \bar{\mathbf{A}}_i^{\dagger} \Delta_i \tag{18}$$

where $\bar{\mathbf{A}}_i^{\dagger} \equiv (\bar{\mathbf{A}}_i^{\mathrm{T}}\bar{\mathbf{A}}_i)^{-1}\bar{\mathbf{A}}_i^{\mathrm{T}}$. Note that in slow operation of the tool platform, the spinning of each leg about its own longitudinal axis is negligible [6]. This assumption leads to the simplified explicit expression for the angular velocity of each leg, ω_{2i}. Taking the cross product of $\mathbf{l}_i$ on both sides of (7) and rearranging the terms, one gets

$$\mathbf{l}_i \times (\omega_{2i} \times \mathbf{l}_i) = \mathbf{l}_i \times [\mathbf{v}_{\mathrm{p}} + (\omega_{\mathrm{p}} \times \mathbf{r}_i) - \dot{\mathrm{d}}_i \mathbf{u}_i] \tag{19}$$

Equation (19) simplifies as

$$\omega_{2i} \equiv \frac{1}{L_i} \Lambda_{li}[\mathbf{v}_{\mathrm{p}} - \Lambda_{ri}\omega_{\mathrm{p}} - \dot{\mathrm{d}}_i \mathbf{u}_i] \tag{20}$$

where $\mathbf{l}_i^{\mathrm{T}} \omega_{2i} = 0$ is used, as it refers to the component of the angular velocity of the ith leg about its longitudinal axis which is neglected.

2.2.2. *Angular acceleration of legs*

Differentiation of (17a) with respect to time yields

$$\bar{\mathbf{A}}_i \dot{\omega}_{2i} = \bar{\Delta}_i \tag{21a}$$

for $i = 1, 2, \ldots, 6$. In (21a), the 4-dimensional vector, $\bar{\Delta}_i$, is given by

$$\bar{\Delta}_i \equiv \begin{bmatrix} \frac{-1}{L_i}[\{\dot{\mathbf{v}}_{\text{p}} - \Lambda_{ri}\dot{\omega}_{\text{p}} + \Lambda_{\text{p}}^2 \mathbf{r}_i - \ddot{\mathrm{d}}_i \mathbf{u}_i\} - \{\Lambda_{2i}(\mathbf{v}_{\text{p}} - \Lambda_{ri}\omega_{\text{p}} - \dot{\mathrm{d}}_i \mathbf{u}_i)\}] \\ [\Lambda_{ui}^2 \Lambda_{li} \omega_{2i}]^{\text{T}} \omega_{2i} \end{bmatrix} \tag{21b}$$

where Λ_{P} and Λ_{2i} are the 3×3 cross-product matrices associated with ω_{P} and ω_{2i}, respectively, and $\ddot{\mathrm{d}}_i$ is the acceleration of slider along the rail of ith chain. Differentiating (7) with respect to time and taking the dot product of $\mathbf{e}_i$ on both sides gives

$$\ddot{\mathrm{d}}_i = \delta_i[\dot{\mathbf{v}}_{\text{p}} - \Lambda_{ri}\dot{\omega}_{\text{p}} + \Lambda_{\text{p}}^2 \mathbf{r}_i - \Lambda_{2i}^2 \mathbf{l}_i]^{\text{T}} \mathbf{e}_i, \text{ where } \delta_i = \frac{1}{\mathbf{e}_i^T \mathbf{u}_i} \tag{21c}$$

Using (21a), the angular acceleration of the ith leg, $\dot{\omega}_{2i}$, is obtained as

$$\dot{\omega}_{2i} = \bar{\mathbf{A}}_i^\dagger \bar{\Delta}_i \tag{22}$$

Similar to the simplified explicit expression of the angular velocity of the ith leg, ω_{2i} of (20), the angular acceleration, $\dot{\omega}_{2i}$, is given from the time differentiation of (20) as

$$\dot{\omega}_{2i} \equiv \frac{1}{L_i} \left[\dot{\Lambda}_{li}\{\mathbf{v}_{\text{p}} - \Lambda_{ri}\omega_{\text{p}} - \dot{\mathrm{d}}_i \mathbf{u}_i\} + \Lambda_{li}\{\dot{\mathbf{v}}_{\text{p}} - \Lambda_{ri}\dot{\omega}_{\text{p}} + \Lambda_{\text{p}}^2 \mathbf{r}_i - \ddot{\mathrm{d}}_i \mathbf{u}_i\} \right] \tag{23}$$

where the 3×3 matrix, $\dot{\Lambda}_{li} \equiv (\omega_{2i} \times \mathbf{e}_i) \times \mathbf{1}$, denotes the time derivative of Λ_{li}.

3. Dynamic Modelling

Following the terminology and basic concepts [8], the uncoupled NE equations of motion necessary for the dynamic modelling of hexaslides are obtained first. The 6-dimensional twist and twist rate vectors of the jth body in the ith chain of the hexaslide, namely, $\mathbf{t}_{ji}$ and $\dot{\mathbf{t}}_{ji}$, respectively, are

$$\mathbf{t}_{ji} \equiv \begin{bmatrix} \omega_{ji}^{\text{T}} & \mathbf{v}_{ji}^{\text{T}} \end{bmatrix}^{\text{T}} \text{ and } \dot{\mathbf{t}}_{ji} \equiv \begin{bmatrix} \dot{\omega}_{ji}^{\text{T}} & \dot{\mathbf{v}}_{ji}^{\text{T}} \end{bmatrix}^{\text{T}} \tag{24a}$$

where the translational velocity and acceleration, namely, $\mathbf{v}_{ji}$ and $\dot{\mathbf{v}}_{ji}$, are associated with mass centre of the jth body in the ith chain. The $6r$-dimensional vectors, r being

the total number of rigid bodies, namely, the *generalized twist* and *generalized twist rate* of the whole system are

$$\mathbf{t} \equiv \begin{bmatrix} \mathbf{t}_{11}^{\mathrm{T}} \cdots \mathbf{t}_{q1}^{\mathrm{T}} \cdots \mathbf{t}_{1n}^{\mathrm{T}} \cdots \mathbf{t}_{qn}^{\mathrm{T}} \ \mathbf{t}_{\mathrm{P}}^{\mathrm{T}} \end{bmatrix}^{\mathrm{T}} \text{ and } \dot{\mathbf{t}} \equiv \begin{bmatrix} \dot{\mathbf{t}}_{11}^{\mathrm{T}} \cdots \dot{\mathbf{t}}_{q1}^{\mathrm{T}} \cdots \dot{\mathbf{t}}_{1n}^{\mathrm{T}} \cdots \dot{\mathbf{t}}_{qn}^{\mathrm{T}} \ \dot{\mathbf{t}}_{\mathrm{P}}^{\mathrm{T}} \end{bmatrix}^{\mathrm{T}} \quad (24b)$$

where $\mathbf{t}_{\mathrm{P}}$ and $\dot{\mathbf{t}}_{\mathrm{P}}$ are the twist and twist rate of the tool platform, respectively; q and n are the number of bodies in each chain and the number of kinematic chains in the hexaslide under study, respectively.

The NE equations of motion for the hexaslide can be put in a compact form as

$$\mathbf{M}\dot{\mathbf{t}} + \mathbf{W}\mathbf{M}\mathbf{t} = \mathbf{w}^{W} + \mathbf{w}^{C} \quad (25a)$$

where the $6(nq + 1) \times 6(nq + 1)$ generalized mass and angular velocity matrices, $\mathbf{M}$ and $\mathbf{W}$, respectively, are expressed as

$$\mathbf{M} \equiv diag \begin{bmatrix} \mathbf{M}_{11}, \cdots, \mathbf{M}_{q1}, \cdots, \mathbf{M}_{1n}, \cdots, \mathbf{M}_{qn}, \mathbf{M}_{\mathrm{p}} \end{bmatrix};$$
$$\mathbf{W} \equiv diag \begin{bmatrix} \mathbf{W}_{11}, \cdots, \mathbf{W}_{q1}, \cdots, \mathbf{W}_{1n}, \cdots, \mathbf{W}_{qn}, \mathbf{W}_{\mathrm{p}} \end{bmatrix} \quad (25b)$$

in which the 6×6 matrices, $\mathbf{M}_{ji}$ and $\mathbf{W}_{ji}$, are the extended mass and extended angular velocity of the jth body in the ith chain, respectively, which are defined by

$$\mathbf{M}_{ji} \equiv \begin{bmatrix} \mathbf{I}_{ji} & \mathbf{O} \\ \mathbf{O} & m_{ji}\mathbf{1} \end{bmatrix}; \text{ and } \mathbf{W}_{ji} \equiv \begin{bmatrix} \Omega_{ji} & \mathbf{O} \\ \mathbf{O} & \mathbf{O} \end{bmatrix} \quad (25c)$$

In (35c), $\mathbf{I}_{ji}, m_{ji}$, and Ω_{ji} are the inertia tensor, mass, and angular velocity matrix associated with ω_{ji}, respectively, of the jth body in the ith chain; whereas $\mathbf{O}$ and $\mathbf{1}$ are the 3×3 null and identity matrices, respectively. The $6(nq + 1)$-dimensional *working* and *nonworking constraint* generalized wrenches, $\mathbf{w}^{W}$ and $\mathbf{w}^{C}$, in (25a) are defined as

$$\mathbf{w}^{W} \equiv \begin{bmatrix} \mathbf{w}_{11}^{W\mathrm{T}} \cdots \mathbf{w}_{q1}^{W\mathrm{T}} \cdots \mathbf{w}_{1n}^{W\mathrm{T}} \cdots \mathbf{w}_{qn}^{W\mathrm{T}} \ \mathbf{w}_{\mathrm{P}}^{W\mathrm{T}} \end{bmatrix}^{\mathrm{T}}, \text{ and}$$
$$\mathbf{w}^{C} \equiv \begin{bmatrix} \mathbf{w}_{11}^{C\mathrm{T}} \cdots \mathbf{w}_{q1}^{C\mathrm{T}} \cdots \mathbf{w}_{1n}^{C\mathrm{T}} \cdots \mathbf{w}_{qn}^{C\mathrm{T}} \ \mathbf{w}_{\mathrm{P}}^{C\mathrm{T}} \end{bmatrix}^{\mathrm{T}} \quad (25d)$$

for $j = 1, 2, \ldots, q; i = 1, 2, \ldots, n$. Note that the working wrench, $\mathbf{w}_{ji}^{W}$, includes the moments and forces due to *actuators*, $\mathbf{w}_{ji}^{a}$, *gravity*, $\mathbf{w}_{ji}^{g}$, *dissipation*, $\mathbf{w}_{ji}^{d}$, and *externally applied*, $\mathbf{w}_{ji}^{e}$. The matrices $\mathbf{M}_{\mathrm{p}}$ and $\mathbf{W}_{\mathrm{p}}$ in (25b) and the wrenches $\mathbf{w}_{\mathrm{p}}^{W}$ and $\mathbf{w}_{\mathrm{p}}^{C}$ in (25d) are related to the tool platform.

3.1. DECOUPLED NATURAL ORTHOGONAL COMPLEMENT MATRICES

The decoupled natural orthogonal complement (DeNOC) matrices, necessary to obtain the set of $n - n$ being the number of independent kinematic chains of the hexaslide under study which is also equals to its DOF—independent dynamic equations of motion, are derived in this section. The latter is obtained here without any complex partial differential equations [6]. Moreover, the use of DeNOC allows one to compute many terms, e.g. $\mathbf{t}_{ji}$, $\dot{\mathbf{t}}_{ji}$, recursively and parallely.

Referring to Figure 3, the twists of the 1st and 2nd moving bodies, namely, slider and leg, of ith kinematic chain of the hexaslide can be expressed as

$$\mathbf{t}_{1i} \equiv \begin{bmatrix} \omega_{1i} \\ \mathbf{v}_{1i} \end{bmatrix} = \mathbf{p}_i \dot{\mathbf{d}}_i \ \text{and} \ \mathbf{t}_{2i} \equiv \begin{bmatrix} \omega_{2i} \\ \mathbf{v}_{2i} \end{bmatrix} = (\mathbf{1} + \bar{\mathbf{C}}_i \bar{\mathbf{D}}_{Ai})\mathbf{t}_{1i} + \bar{\mathbf{C}}_i \bar{\mathbf{D}}_{Pi} \mathbf{t}_P \qquad (26a)$$

where the 6-dimensional vector, $\mathbf{p}_i$, and the 6×3 matrix, $\bar{\mathbf{C}}_i$, are defined as

$$\mathbf{p}_i \equiv \begin{bmatrix} \mathbf{0} \\ \mathbf{u}_i \end{bmatrix}; \bar{\mathbf{C}}_i \equiv \begin{bmatrix} \mathbf{1} \\ \Lambda_{ci} \end{bmatrix} \qquad (26b)$$

In (26b), the 3×3 cross-product matrix, Λ_{ci}, is associated with the vector, $\mathbf{l}_{ci}$, shown in Figure 3, and the 3×6 matrices $\bar{\mathbf{D}}_{Ai}$ and $\bar{\mathbf{D}}_{Pi}$ in (26a) are given by

$$\bar{\mathbf{D}}_{Ai} = \tilde{\mathbf{A}}_i^\dagger \mathbf{D}_{Ai}; \ \textit{and} \ \bar{\mathbf{D}}_{Pi} = \tilde{\mathbf{A}}_i^\dagger \mathbf{D}_{Pi} \qquad (26c)$$

In (26c), the 4×6 matrices $\mathbf{D}_{Ai}$ and $\mathbf{D}_{Pi}$ are given by

$$\mathbf{D}_{Ai} = \frac{1}{\mathrm{L}_i} \begin{bmatrix} \mathbf{O} & \mathbf{1} \\ \mathbf{0}^\mathrm{T} & \mathbf{0}^\mathrm{T} \end{bmatrix}; \ \text{and} \ \mathbf{D}_{Pi} = \frac{1}{\mathrm{L}_i} \begin{bmatrix} \Lambda_{ri} & -\mathbf{1} \\ \mathbf{0}^\mathrm{T} & \mathbf{0}^\mathrm{T} \end{bmatrix} \qquad (26d)$$

Note that $\mathbf{0}$ of (26b) and (26d) refers to the 3-dimensional null vector. It may also be noted that when simplified expression of the leg angular velocity, ω_{2i}, given by (20) is used, $\bar{\mathbf{D}}_{Ai}$ and $\bar{\mathbf{D}}_{Pi}$ of (26a) take the following form, instead of those given by (26c):

$$\bar{\mathbf{D}}_{Ai} = \frac{1}{\mathrm{L}_i} \begin{bmatrix} \mathbf{O} & -\Lambda_{li} \end{bmatrix}; \ \text{and} \ \bar{\mathbf{D}}_{Pi} = \frac{1}{\mathrm{L}_i} \Lambda_{li} \begin{bmatrix} -\Lambda_{ri} & \mathbf{1} \end{bmatrix} \qquad (26e)$$

Since each kinematic chain of the hexaslide has two bodies, namely, the slider and leg, respectively, there are only two recursive expressions given in (26a). For each chain, another 12-dimensional vector, namely, the *chain-twist*, $\bar{\mathbf{t}}_i$, is then introduced as

$$\bar{\mathbf{t}}_i \equiv \begin{bmatrix} \mathbf{t}_{1i}^\mathrm{T} & \mathbf{t}_{2i}^\mathrm{T} \end{bmatrix}^\mathrm{T} = \mathbf{P}_{Pi} \mathbf{t}_P + \mathbf{P}_{Ai} \mathbf{p}_i \dot{\mathbf{d}}_i \qquad (27a)$$

where the 12×6 matrices, $\mathbf{P}_{\mathrm{P}i}$ and $\mathbf{P}_{\mathrm{A}i}$ are given by

$$\mathbf{P}_{\mathrm{P}i} \equiv \begin{bmatrix} \mathbf{O} \\ \bar{\mathbf{P}}_{\mathrm{P}i} \end{bmatrix}; \mathbf{P}_{\mathrm{A}i} \equiv \begin{bmatrix} \mathbf{1} \\ \bar{\mathbf{P}}_{\mathrm{A}i} \end{bmatrix} \tag{27b}$$

in which $\bar{\mathbf{P}}_{\mathrm{A}i} \equiv \mathbf{1} + \bar{\mathbf{C}}_i \bar{\mathbf{D}}_{\mathrm{A}i}$, and $\bar{\mathbf{P}}_{\mathrm{P}i} \equiv \bar{\mathbf{C}}_i \bar{\mathbf{D}}_{\mathrm{P}i}$. The generalized twist of the hexaslide, $\mathbf{t}$ of (24b), is then written from (27b), for $i = 1, 2, \ldots, n$, as

$$\mathbf{t} \equiv \mathbf{P}_{\mathrm{P}} \mathbf{t}_{\mathrm{P}} + \mathbf{P}_{\mathrm{A}} \mathbf{T}_{\mathrm{d}} \dot{\mathbf{d}} \tag{28a}$$

where the $6(nq + 1)$-dimensional vector, $\mathbf{t}$, is defined as

$$\mathbf{t} \equiv \begin{bmatrix} \bar{\mathbf{t}}_1^{\mathrm{T}} \cdots \bar{\mathbf{t}}_n^{\mathrm{T}} \mathbf{t}_{\mathrm{P}}^{\mathrm{T}} \end{bmatrix}^{\mathrm{T}}; \text{ where } \bar{\mathbf{t}}_i \equiv \begin{bmatrix} \mathbf{t}_{1i}^{\mathrm{T}} \cdots \mathbf{t}_{qi}^{\mathrm{T}} \end{bmatrix}^{\mathrm{T}} \tag{28b}$$

Moreover, the $6(nq + 1) \times 6$ matrix, $\mathbf{P}_{\mathrm{P}}$, the $6(nq + 1) \times 6n$ matrix, $\mathbf{P}_{\mathrm{A}}$, the $6n \times n$ matrix, $\mathbf{T}_{\mathrm{d}}$, and the n-dimensional joint rate vector, $\dot{\mathbf{d}}$, are given by

$$\mathbf{P}_{\mathrm{P}} \equiv \begin{bmatrix} \mathbf{P}_{\mathrm{P}1} \\ \cdot \\ \cdot \\ \cdot \\ \mathbf{P}_{\mathrm{P}n} \\ \mathbf{1} \end{bmatrix}; \mathbf{P}_{\mathrm{A}} \equiv \begin{bmatrix} \mathbf{P}_{\mathrm{A}1} & & \mathbf{O} \\ & \cdot & \\ & & \cdot \\ & & & \cdot \\ \mathbf{O} & & \mathbf{P}_{\mathrm{A}n} \\ \mathbf{O} & & \mathbf{O} \end{bmatrix}; \mathbf{T}_{\mathrm{d}} \equiv \begin{bmatrix} \mathbf{p}_1 & & \mathbf{0} \\ & \cdot & \\ & & \cdot \\ & & & \cdot \\ \mathbf{0} & & \mathbf{p}_n \end{bmatrix}; \text{ and } \dot{\mathbf{d}} \equiv \begin{bmatrix} \dot{\mathrm{d}}_1 \\ \cdot \\ \cdot \\ \cdot \\ \dot{\mathrm{d}}_n \end{bmatrix} \tag{28c}$$

Note that for the hexaslide under study, $n = 6$ and $q = 2$. Hence, in (28c), $\mathbf{P}_{\mathrm{P}}$, $\mathbf{P}_{\mathrm{A}}$, and $\mathbf{T}_{\mathrm{d}}$ are the 78×6, 78×36, 36×6 matrices, respectively, whereas $\dot{\mathbf{d}}$ is the 6-dimensional vector. Also, from (9), the twist of the tool platform, $\mathbf{t}_{\mathrm{P}}$, can be expressed as

$$\mathbf{t}_{\mathrm{P}} = \mathbf{J}_{\mathrm{t}}^{-1} \mathbf{J}_{\mathrm{a}} \dot{\mathbf{d}} \tag{29}$$

where the 6×6 matrices, $\mathbf{J}_{\mathrm{t}}$ and $\mathbf{J}_{\mathrm{a}}$, are given in (10). In (29), the matrix $\mathbf{J}_{\mathrm{a}}$ is rewritten as

$$\mathbf{J}_{\mathrm{a}} = \mathbf{P}_l \mathbf{T}_{\mathrm{d}}, \text{ where } \mathbf{P}_l \equiv \mathrm{diag}[\, \mathbf{p}_{l1}^{\mathrm{T}} \cdots \mathbf{p}_{ln}^{\mathrm{T}} \,] \tag{30}$$

in which the 6-dimensional vector, $\mathbf{p}_{li} \equiv \begin{bmatrix} \mathbf{0}^{\mathrm{T}} \mathbf{e}_i^{\mathrm{T}} \end{bmatrix}^{\mathrm{T}}$, for $i = 1, 2, \ldots, n$. Substituting (30) into (28a), the generalized twist, $\mathbf{t}$, is rewritten as

$$\mathbf{t} = \mathbf{T} \dot{\mathbf{d}}, \text{ where } \mathbf{T} \equiv \mathbf{T}_{\mathrm{h}} \mathbf{T}_{\mathrm{d}} \tag{31a}$$

wherein the $6(nq + 1) \times 6n$ or the 78×36 matrix, for $n = 6$ and $q = 2$, $\mathbf{T}_{\mathrm{h}}$, is given as

$$\mathbf{T}_{\mathrm{h}} \equiv \mathbf{P}_{\mathrm{P}} \mathbf{J}_{\mathrm{t}}^{-1} \mathbf{P}_l + \mathbf{P}_{\mathrm{A}} \tag{31b}$$

In (31a), the $6(nq + 1) \times 6$ matrix, $\mathbf{T}$, is nothing but the NOC matrix of the hexaslide, whereas the $6(nq + 1) \times 6n$ matrix, $\mathbf{T}_h$, and the $6n \times n$ matrix, $\mathbf{T}_d$, are the DeNOC matrices. Note that, the DeNOC matrices for the hexaslide, are full block, $\mathbf{T}_h$, and block diagonal, $\mathbf{T}_d$. Saha and Schiehlen [25] showed that a closed-loop parallel-chain system has three DeNOC matrices, which is not the case here. This is due to the fact that, in [25], the moving platform was divided into several parts. Each part was then considered as the last body of a serial-chain. As a result, a lower block triangular matrix, similar to the serial-chain system, could be extracted. Such formulation for the hexalides under study would require the information on the joint angles, rates and accelerations of the unactuated joints, which otherwise are not required. So, an alternate approach is followed, where the twists of all the bodies are expressed in terms of the twist of the moving platform and the joint rates.

3.2. COUPLED DYNAMIC EQUATIONS

As in [18], pre-multiplication of $\mathbf{T}^T$ to the uncoupled NE equations, (25a), leads to

$$\mathbf{T}^T(\mathbf{M}\dot{\mathbf{t}} + \mathbf{W}\mathbf{M}\mathbf{t}) = \mathbf{T}^T(\mathbf{w}^W + \mathbf{w}^C), \text{ where } \mathbf{T} \equiv \mathbf{T}_h\mathbf{T}_d \tag{32}$$

In (32), $\mathbf{T}^T\mathbf{w}^C = 0$, as the constraint wrenches do not perform any work. Upon substitution of $\mathbf{t} = \mathbf{T}\dot{\mathbf{d}}$, $\dot{\mathbf{t}} = \dot{\mathbf{T}}\dot{\mathbf{d}} + \mathbf{T}\ddot{\mathbf{d}}$, and $\dot{\mathbf{T}}_d = \mathbf{O}$, (32) takes the form

$$\mathbf{I}\ddot{\mathbf{d}} + \mathbf{C}\dot{\mathbf{d}} = \tau \tag{33}$$

where $\mathbf{I} = \mathbf{T}_d^T\tilde{\mathbf{M}}\mathbf{T}_d$: the $n \times n$ generalized inertia matrix (GIM) of the hexaslide system at hand; $\mathbf{C} = \mathbf{T}_d^T(\tilde{\mathbf{M}}_d + \tilde{\mathbf{M}}_h)\mathbf{T}_d$: the $n \times n$ generalized matrix of convective inertia terms; and $\tau = \mathbf{T}_d^T\tilde{\mathbf{w}}^W$: the n-dimensional vector of generalized forces due to actuators, gravity and other external moments and forces. The $6n \times 6n$ matrices, $\tilde{\mathbf{M}}$, $\tilde{\mathbf{M}}_d$, $\tilde{\mathbf{M}}_h$ and the $6n$-dimensional vector, $\tilde{\mathbf{w}}^W$, are expressed as

$$\tilde{\mathbf{M}} = \mathbf{T}_h^T\mathbf{M}\mathbf{T}_h; \ \tilde{\mathbf{M}}_d = \mathbf{T}_h^T\mathbf{M}\dot{\mathbf{T}}_h; \ \tilde{\mathbf{M}}_h = \mathbf{T}_h^T\mathbf{W}\mathbf{M}\mathbf{T}_h; \text{ and } \tilde{\mathbf{w}}^W = \mathbf{T}_h^T\mathbf{w}^W \tag{34}$$

Furthermore, each element of the matrices and vectors of (33) can be written explicitly. For example, the (i, j) element of the GIM, i.e., i_{ij}, is given by

$$i_{ij} = \mathbf{p}_i^T\tilde{\mathbf{M}}_{ij}\mathbf{p}_j \tag{35}$$

where the 6×6 symmetric matrix, $\tilde{\mathbf{M}}_{ij}$, can be computed as

$$\tilde{\mathbf{M}}_{ij} = \mathbf{M}_{1j} + \left(\sum_{k=1}^{n}\mathbf{H}_{ki}^T\mathbf{M}_{2k}\mathbf{H}_{kj}\right) + \mathbf{H}_{Pi}^T\mathbf{M}_P\mathbf{H}_{Pj} \quad \text{for} \quad i = j \tag{36a}$$

$$= \left(\sum_{k=1}^{n} \mathbf{H}_{ki}^{\mathrm{T}} \mathbf{M}_{2k} \mathbf{H}_{kj} \right) + \mathbf{H}_{\mathrm{P}i}^{\mathrm{T}} \mathbf{M}_{\mathrm{P}} \mathbf{H}_{\mathrm{P}j} \quad \text{for} \quad i \neq j \tag{36b}$$

In (36), the 6×6 matrices, $\mathbf{M}_{2k}$ and $\mathbf{M}_{\mathrm{P}}$ are the mass matrices for the 2nd body, i.e., leg, of the kth chain and the tool platform, respectively. The 6×6 matrices, $\mathbf{H}_{kj}$ and $\mathbf{H}_{\mathrm{P}i}$, are the block elements of matrix $\mathbf{T}_{\mathrm{h}}$. Equation (33) is nothing but the n-independent EL equations of motion, which are obtained without any complex partial differentiation.

4. Inverse Dynamics Algorithm

An inverse dynamics algorithm, useful for power estimation of the actuator motors, control and others, is presented here. In inverse dynamics, the tool platform motions are given as input to find all the actuator forces, i.e., vector τ of (33). The matrices, $\mathbf{I}$, $\mathbf{C}$, etc., need not be calculated explicitly. These are, however, useful for the forward dynamics [25, 26]. The following is proposed inverse dynamics scheme:

S-1: Solve the inverse kinematics to obtain d_i, $\dot{d}_i$, and $\ddot{d}_i$.

S-2: Calculate the twist and twist rates of all the bodies $\mathbf{t}_{ji}$ and $\dot{\mathbf{t}}_{ji}$ recursively.

S-3: Find the matrices $\mathbf{M}_{ji}$, $\mathbf{M}_{\mathrm{P}}$, $\mathbf{W}_{ji}$ and $\mathbf{W}_{\mathrm{P}}$.

S-4: Compute the 6-dimensional wrenches, $\mathbf{w}_{ji}$ and $\mathbf{w}_{\mathrm{P}}$ of (25d), as

$$\mathbf{w}_{ji} = \mathbf{M}_{ji} \dot{\mathbf{t}}_{ji} + \mathbf{W}_{ji} \mathbf{M}_{ji} \mathbf{t}_{ji} - \mathbf{w}_{ji}^{g} - \mathbf{w}_{ji}^{d} - \mathbf{w}_{ji}^{e}; \text{ and}$$

$$\mathbf{w}_{\mathrm{P}} = \mathbf{M}_{\mathrm{P}} \dot{\mathbf{t}}_{\mathrm{P}} + \mathbf{W}_{\mathrm{P}} \mathbf{M}_{\mathrm{P}} \mathbf{t}_{\mathrm{P}} - \mathbf{w}_{\mathrm{P}}^{g} - \mathbf{w}_{\mathrm{P}}^{d} - \mathbf{w}_{\mathrm{P}}^{e} \tag{37}$$

S-5: Find the DeNOC matrices in two stages, namely,

(i) The generalized twist, $\mathbf{t}$, is related with dependent generalized velocities, $\dot{\psi}$, as

$$\mathbf{t} \equiv \bar{\mathbf{T}}_{\mathrm{h}} \bar{\mathbf{T}}_{\mathrm{d}} \dot{\psi} \quad \text{where} \quad \dot{\psi} \equiv \begin{bmatrix} \dot{\mathbf{d}}^{\mathrm{T}} & \mathbf{t}_{\mathrm{P}}^{\mathrm{T}} \end{bmatrix}^{\mathrm{T}} \tag{38a}$$

In (38a), $\bar{\mathbf{T}}_{\mathrm{h}}$ and $\bar{\mathbf{T}}_{\mathrm{d}}$ are the $6(nq + 1) \times 6(n + 1)$ and $6(n + 1) \times (n + 6)$ DeNOC matrices with respect to the dependent generalized velocities, $\dot{\psi}$, given as

$$\bar{\mathbf{T}}_{\mathrm{h}} \equiv \begin{bmatrix} \begin{bmatrix} \mathbf{1} \\ \bar{\mathbf{P}}_{\mathrm{A}1} \end{bmatrix} & \begin{bmatrix} \mathbf{O} \\ \mathbf{O} \end{bmatrix} & \begin{bmatrix} \mathbf{O} \\ \bar{\mathbf{P}}_{\mathrm{P}1} \end{bmatrix} \\ & \ddots & \vdots \\ \begin{bmatrix} \mathbf{O} \\ \mathbf{O} \end{bmatrix} & \begin{bmatrix} \mathbf{1} \\ \bar{\mathbf{P}}_{\mathrm{A}n} \end{bmatrix} & \begin{bmatrix} \mathbf{O} \\ \bar{\mathbf{P}}_{\mathrm{P}n} \end{bmatrix} \\ \mathbf{O} & \cdots \quad \mathbf{O} & \mathbf{1} \end{bmatrix} ; \text{ and } \bar{\mathbf{T}}_{\mathrm{d}} \equiv \begin{bmatrix} \mathbf{p}_1 & & \mathbf{0} \ \mathbf{O} \\ & \ddots & \vdots \\ \mathbf{0} & \mathbf{p}_n & \mathbf{O} \\ \mathbf{0} & \cdots \ \mathbf{0} & \mathbf{1} \end{bmatrix} \tag{38b}$$

in which $\mathbf{0}^s$, $\mathbf{O}^s$, and $\mathbf{1}^s$ refer to the 6-dimensional null vectors, the 6×6 null matrices, and the 6×6 identity matrices, respectively.

(ii) The dependent generalized velocities, $\dot{\psi}$, are related with the independent joint rates, $\dot{\mathbf{d}}$, as

$$\dot{\psi} = \mathbf{T}_n \dot{\mathbf{d}}, \text{ where the } (n+6) \times n \text{ matrix, } \mathbf{T}_n \equiv \begin{bmatrix} \mathbf{1} \\ \mathbf{J}^{-1} \end{bmatrix} \tag{39}$$

Note that, $\mathbf{T} = \bar{\mathbf{T}}_h \bar{\mathbf{T}}_d \mathbf{T}_n = \mathbf{T}_h \mathbf{T}_d$. Hence, the DeNOC matrices are obtained here in two stages, as a multiplication of three block matrices, $\bar{\mathbf{T}}_h$, $\bar{\mathbf{T}}_d$, and $\mathbf{T}_n$. Hence, premultiplication of $\mathbf{T}^T$ with the uncoupled equations of motion, (25a), produces the required actuator forces, $\tau^a = \mathbf{T}^T \mathbf{w}$.

S-6: Compute the 6-dimensional vectors, $\tau^{(I)}$ and $\bar{\mathbf{w}}_{2i}$, which are associated with the resultant vector obtained from the premultiplication of the DeNOC matrices with respect to the dependent joint rate vector, $\dot{\psi}$, (38a), with the uncoupled NE equation, (25a), i.e., $\bar{\mathbf{T}}_d^T \bar{\mathbf{T}}_h^T \mathbf{w}$, where the elements of the generalized wrench, $\mathbf{w}$ defined similar to (25d), are evaluated in Step-4. Vectors $\tau^{(I)}$ and $\bar{\mathbf{w}}_{2i}$ are defined as

$$\tau^{(I)} = \begin{bmatrix} \tau_1^{(I)} \cdots \tau_6^{(I)} \end{bmatrix}^T, \text{ and } \bar{\mathbf{w}}_{2i} = \bar{\mathbf{P}}_{Pi}^T \mathbf{w}_{2i} \tag{40}$$

where $\tau_i^{(I)} = \mathbf{p}_i^T (\mathbf{w}_{1i} + \bar{\mathbf{P}}_{Ai}^T \mathbf{w}_{2i})$ for $i = 1, 2, \ldots, 6$.

S-7: Compute the 6-dimensional vector, $\tau^{(II)}$, as a part of the vector resulting from the multiplication of $\mathbf{T}_n^T$ with the vector obtained from the premultiplication of the transpose of the DeNOC matrices associated with the dependent joint rate vector with the uncoupled NE equations of motion, i.e.,

$$\tau^{(II)} = \mathbf{J}_a^T \mathbf{J}_t^{-T} \left(\mathbf{w}_P + \sum_{i=1}^{6} \bar{\mathbf{w}}_{2i} \right) \tag{41}$$

S-8: Compute the 6-dimensional vector consisting of the actuator forces, τ_i^a, as

$$\tau^a = \tau^{(I)} + \tau^{(II)} \tag{42}$$

The above relations allow parallel computations similar to that reported in [13]. The scheme of parallel computations is shown in Figure 4. The complexity of the proposed algorithm is linear in terms of the total number of bodies, r, i.e., $O(r)$. The algorithm is implemented in MATLAB. Even though the proposed algorithm is suitable for the parallel computations, it could not be practically realized due to the non-availability of suitable software and hardware to connect several computers to run parallel.
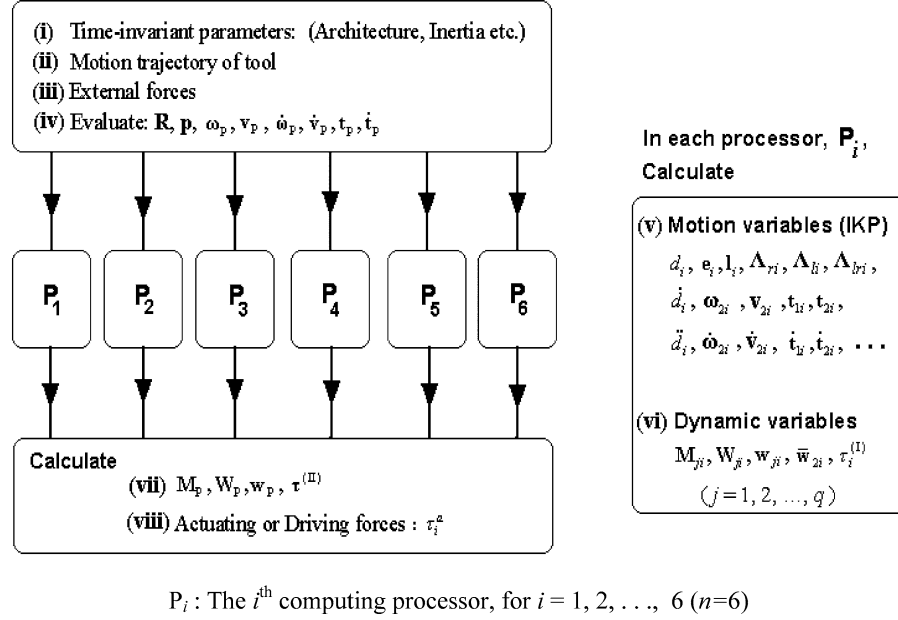
(i)   Time-invariant parameters: (Architecture, Inertia etc.)
(ii) Motion trajectory of tool
(iii) External forces
(iv) Evaluate: $\mathbf{R}, \mathbf{p}, \omega_p, v_p, \dot{\omega}_p, \dot{v}_p, t_p, \dot{t}_p$

In each processor, P_i, Calculate

(v) Motion variables (IKP)
$d_i, e_i, l_i, \Lambda_{ri}, \Lambda_{li}, \Lambda_{hi},$
$\dot{d}_i, \omega_{2i}, v_{2i}, t_{1i}, t_{2i},$
$\ddot{d}_i, \dot{\omega}_{2i}, \dot{v}_{2i}, \dot{t}_{1i}, \dot{t}_{2i}, \ldots$

(vi) Dynamic variables
$\mathbf{M}_{ji}, \mathbf{W}_{ji}, \mathbf{w}_{ji}, \bar{\mathbf{w}}_{2i}, \tau_i^{(I)}$
$(j = 1, 2, \ldots, q)$

Calculate
(vii) $M_p, W_p, w_p, \tau^{(II)}$
(viii) Actuating or Driving forces : τ_i^a

P_i : The ith computing processor, for $i = 1, 2, \ldots, 6$ ($n=6$)

Figure 4. Parallel computations for the inverse dynamics algorithm.

5. An Illustration: Circular Contouring of the HexaM

An illustration of the invese dynamics algorithm proposed in Section 4 is presented here considering an existing machine tool based on hexaslides, namely, the HexaM [4, 15, 27]. The architecture of the HexaM is shown in Figure 5, whose geometric parameters are given in Table I. Note that, each column on the right hand sides of the vectors $\mathbf{a}_i$, $\bar{\mathbf{e}}_i$, and $\mathbf{r}_i'$, in Table I, represent the three position coordinates of point A_i in fixed frame, point E_i in fixed frame, and point B_i in the moving frame, respectively, for $i = 1, 2, \ldots, 6$.

The mass and inertia properties, taken from Kim and Ryu [15] for the comparison of inverse dynamics results, are:

- Mass of each slider, $m_s = 0.9963$ kg
- Mass of each leg, $m_l = 2.1729$ kg
- Mass of the platform, $m_p = 10.7673$ kg
- Mass moment of inertia of the tool platform about its centroidal axes, i.e., $\bar{\mathbf{I}}_P$, $\bar{\mathbf{I}}_P = diag$ [0.118, 0.118, 0.236] kg-m^2
- Mass moment of inertia of each leg about its centroidal axes, i.e., $\bar{\mathbf{I}}_l$, $\bar{\mathbf{I}}_l = diag$ [0.140, 0.140, 0.000] kg-m^2
- Acceleration due to gravity, g $= 9.81$ m/s^2
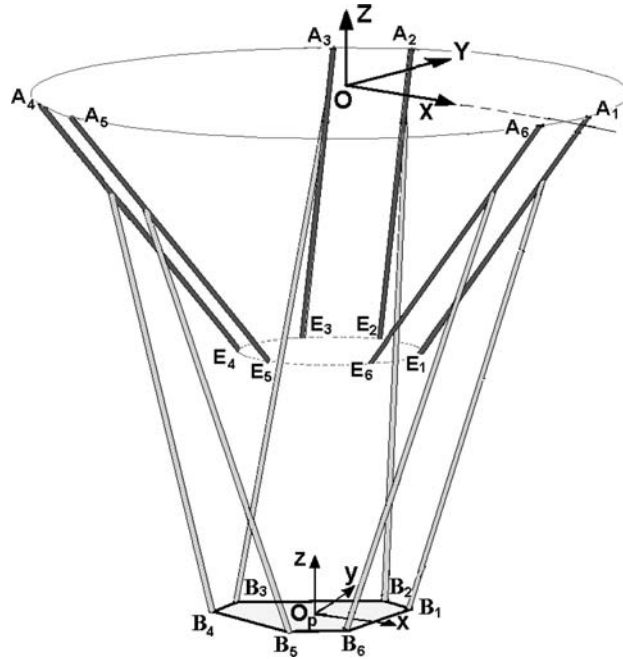- Length of each leg, i.e., L_i for $i = 1, 2, \ldots, 6$, namely, $L = 0.9$ m.

Figure 5. The kinematic sketch of HexaM.

Table I. Geometric Parameters of The HexaM

i		1	2	3	4	5	6
$\mathbf{a}_i \equiv \begin{bmatrix} a_{iX} \\ a_{iY} \\ a_{iZ} \end{bmatrix}$		$\begin{bmatrix} 0.9157 \\ 0.1100 \\ 0.0000 \end{bmatrix}$	$\begin{bmatrix} -0.3625 \\ 0.8480 \\ 0.0000 \end{bmatrix}$	$\begin{bmatrix} -0.5531 \\ 0.7380 \\ 0.0000 \end{bmatrix}$	$\begin{bmatrix} -0.5531 \\ -0.7380 \\ 0.0000 \end{bmatrix}$	$\begin{bmatrix} -0.3625 \\ -0.8480 \\ 0.0000 \end{bmatrix}$	$\begin{bmatrix} 0.9157 \\ -0.1100 \\ 0.0000 \end{bmatrix}$
$\bar{\mathbf{e}}_i \equiv \begin{bmatrix} \bar{e}_{iX} \\ \bar{e}_{iY} \\ \bar{e}_{iZ} \end{bmatrix}$		$\begin{bmatrix} 0.3095 \\ 0.1100 \\ -0.3500 \end{bmatrix}$	$\begin{bmatrix} -0.0594 \\ 0.3230 \\ -0.3500 \end{bmatrix}$	$\begin{bmatrix} -0.2500 \\ 0.2130 \\ -0.3500 \end{bmatrix}$	$\begin{bmatrix} -0.2500 \\ -0.2130 \\ -0.3500 \end{bmatrix}$	$\begin{bmatrix} -0.0594 \\ -0.3230 \\ -0.3500 \end{bmatrix}$	$\begin{bmatrix} 0.3095 \\ -0.1100 \\ -0.3500 \end{bmatrix}$
$\mathbf{r}'_i \equiv \begin{bmatrix} r'_{iX} \\ r'_{iY} \\ r'_{iZ} \end{bmatrix}$		$\begin{bmatrix} 0.1100 \\ 0.1229 \\ 0.0000 \end{bmatrix}$	$\begin{bmatrix} 0.1615 \\ 0.0337 \\ 0.0000 \end{bmatrix}$	$\begin{bmatrix} 0.0515 \\ -0.1567 \\ 0.0000 \end{bmatrix}$	$\begin{bmatrix} -0.0515 \\ -0.1567 \\ 0.0000 \end{bmatrix}$	$\begin{bmatrix} -0.1615 \\ 0.0337 \\ 0.0000 \end{bmatrix}$	$\begin{bmatrix} -0.1100 \\ 0.1229 \\ 0.0000 \end{bmatrix}$

The tool trajectory, as shown in Figure 6, is taken as

- Circular contour on the XY-plane with uniform speed, N = 40 rpm about Z-axis
- Radius of circle, R_c = 0.1 m
- Coordinates of the circle center, $C_c = (p_X, p_Y, p_Z) = (0, 0, -0.11)$
- Position vector of the center of tool platform with reference to the origin of fixed frame, $\mathbf{p} \equiv \begin{bmatrix} p_X + R_C \cos\theta & p_Y + R_C \sin\theta & p_Z \end{bmatrix}^T$, where '$\theta$' is the angular position of the tool center point (TCP) with respect to reference axis, as shown in Figure 6.
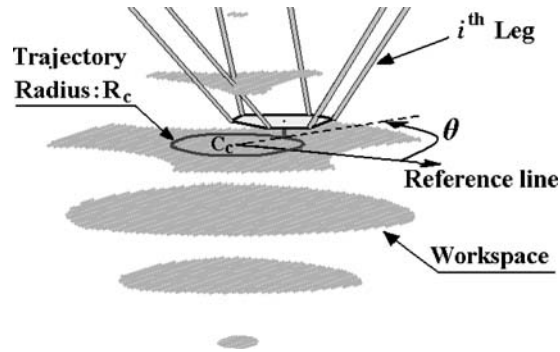
Figure 6. Schematic depicting the circular trajectory.

In order to validate the inverse dynamics results, the dissipative and external wrenches on the tool platform at the TCP are not considered similar to that in [15]. The actuator or the controlling forces obtained using the proposed inverse dynamics algorithm are shown in Figure 7, which exactly match with those reported in [15]. The actuator forces are also obtained using the numerical NOC calculation, as in [22] for the hexapods. The maximum deviation in the results is in the order of 10^{-12} N, which is negligible. Even though the results from the proposed DeNOC and the numerical NOC based algorithms are same, the advantages of the former lie in its faster $O(r)$ computational complexities. Using the single processor, the DeNOC based inverse dynamics algorithm took only 4s in a P IV processor-1.8 GHz, whereas the numerical NOC [22] took 6.8s. This is obvious since a total of $O(nr)$ computations will be required to find the complete NOC.

6. Effect of Leg and Slider Inertias

In order to simplify the dynamic model of hexaslides, the researchers tend to neglect the mass and inertia of the sliders and or legs. An attempt is made, in this section, to study the effect of the leg and slider inertias. The actuator forces are found considering with and without the leg and slider inertias. The following three cases are studied:

Case 1: Consider tool platform and leg, i.e., neglect only slider inertias;

Case 2: Consider tool platform and slider, i.e., neglect only leg inertias; and

Case 3: Consider only tool platform inertia, i.e., neglect both the leg and slider inertias.

All the above three cases are compared with those when the inertias of all the bodies, i.e., the tool platform, legs and sliders, are considered. For this investigation, the HexaM with the geometric and inertia properties same as that in Section 5 is considered. The tool trajectory is also taken same as that considered in Section 5. The variation of the actuator forces due to the inertia of various bodies when the operating speed of the tool platform is 40rpm is shown in Figure 8. It may be noted
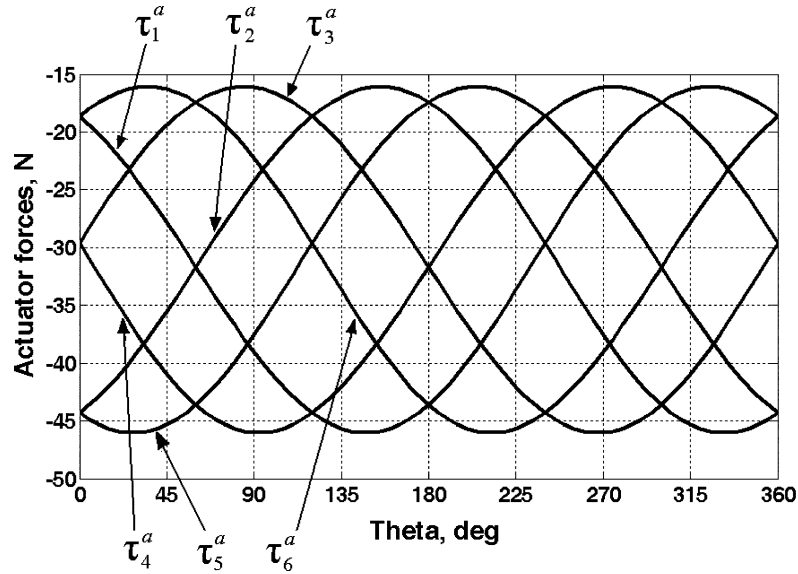
Figure 7. Actuator forces during circular contouring.

that the influence of the leg inertia on the actuator forces is more when compared to the slider inertia. The same is evident even from the plot of the maximum difference in the actuator forces, Figure 9. The difference in the actuator forces for Case 1 is computed as the differences in the actuator forces while the slider inertia is neglected from those considering the inertias of all the bodies. It may also be observed that the maximum difference in the actuator forces increase drastically at higher speeds of the tool platform for all the three cases of study. Moreover, there are significant differences in the actuator forces for all the three cases even at relatively low speed, $N = 40$ rpm. Hence, it is advisable not to neglect the slider and leg inertias while computing the actuator forces for the hexaslides.

7. Conclusions

In this paper, dynamic model of a general hexaslide based on the decoupled natural orthogonal complement (DeNOC) matrices is proposed. All the moving bodies, including the sliders of the hexaslide are considered during the dynamic analysis. The DeNOC matrices of hexaslides offer the following features: (i) Natural development of parallel inverse dynamics algorithm; (ii) Explicit analytical expressions for the generalized inertia matrix (GIM) and others that are useful for debugging, and checking the effects of mass and inertias of the sliders or legs; (iii) Recursive forward dynamics algorithms, as shown in [25]. It is shown how the proposed inverse dynamics algorithm perform better compared to the numerical evaluation of
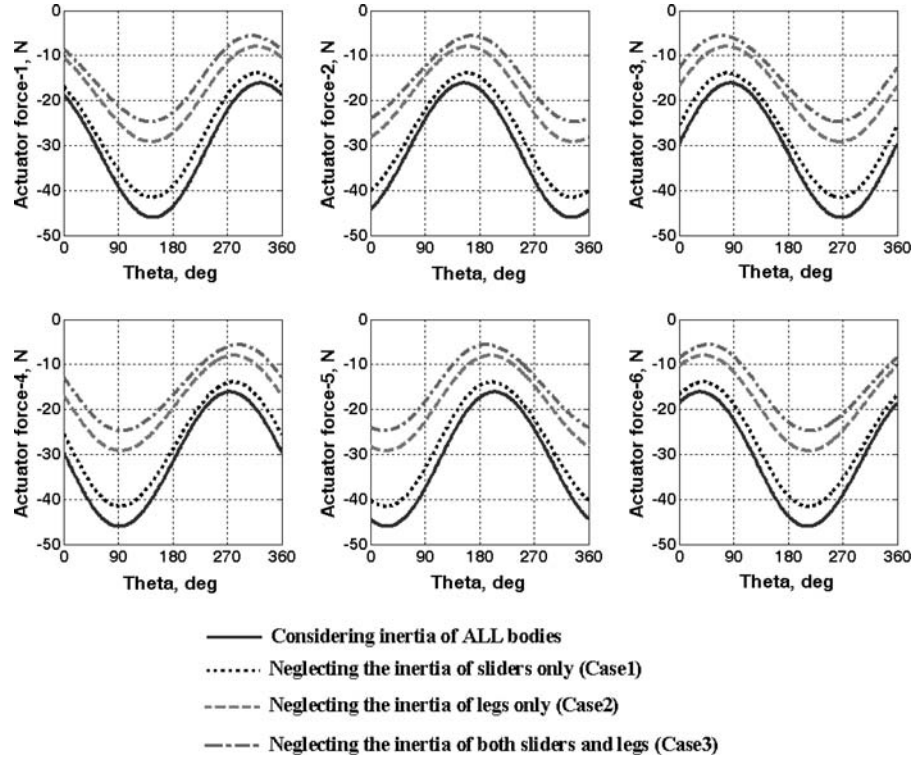
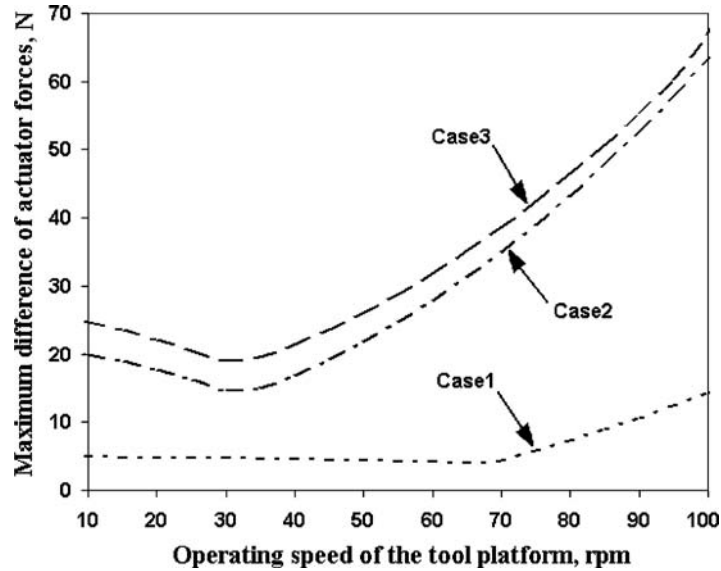*Figure 8*. Effect of different inertia on actuator forces ($N = 40$ rpm).

Figure 9. Variation in maximum difference of actuator forces.

the NOC matrix. The inverse dynamics for the HexaM is carried out implementing the proposed algorithm while its TCP performs a circular contouring. The agreement in the results with those reported in [16] validates the proposed algorithm. The actuator forces obtained are useful for the design of a hexaslide where its motor specifications are required for an application. Besides, the model can be used for the dynamics based control purposes. Secondly, the effect of leg and slider inertias is also studied, which clearly suggests that neither of these can be neglected while finding the actuator forces.

Acknowledgments

References

1. Stewart, D., A platform with six degrees of freedom, *Proc. Instn. of Mechanical Engineers*, (Part-I), **180**(15), 1965, 371–386.
2. Boër, C. R., Molinori-Tosatti L. and Smith, K. S., *Parallel Kinematic Machines: Theoretical Aspects and Industrial Requirements*, Springer-Verlag, London, 1999.
3. Honegger, M., Codourey, A. and Burdet, E., 'Adaptive control of the Hexaglide, a 6 DOF parallel manipulator', *Proc. of IEEE- ICRA 97*, Albuquerque, 1997, 543–548.
4. Suzuki, M., Watanabe, K., Shibukawa, T., Tooyama, T. and Hattori, K., 'Development of milling machine with parallel mechanism', *Toyota Technical Review*, **47**(1), 1997, 125–130.
5. Pritschow, G. and Wurst, K. H., 'Systematic design of Hexapods and parallel link systems', *Annals of the CIRP*, **46**(1), 1997, 291–295.
6. Tsai, L-W., *Robot Analysis*, John Wiley & Sons, Inc., New York, 1999.
7. Merlet, J. P., *Parallel Robots*, Kluwer Academic Publishers, The Netherlands, 2000.
8. Angeles, J., *Fundamentals of Robotic Mechanical Systems*, Springer-Verlag, New York, 2003.
9. Hollerbach, J. M., 'A recursive Lagrangian formulation of manipulator dynamics and a comparative study of dynamics formulation complexity', *IEEE Trans. on Sys., Man, and Cybernatics*, V. SMC-10, 1980, 730–736.
10. Nakamura, Y. and Ghodoussi, M., 'Dynamic computation of closed-link robot mechanisms with nonredundant and redundant actuators', *IEEE Trans. on Robotics and Auto.*, **5**(3), 1989, 294–302.
11. Geng, Z., Haynes, L. S., Lee, J. D. and Carroll, R., L., 'On the dynamic model and kinematic analysis of a class of Stewart platforms', *Robotics and Autonomous Systems*, **9**, 1992, 237–254.
12. Dasgupta B. and Mruthyunjaya, T.S., 'A Newton-Euler formulation for the inverse dynamics of the Stewart platform manipulator', *Mechanism and Machine Theory*, **33**(8), 1998, 1135–1152.
13. Gosselin, C. M., 'Parallel computation algorithms for the kinematics and dynamics of parallel manipulators', *Trans. ASME, J. of Dynamic Systems Measurement and Control*, **118**(1), 1996.
14. Kim, J. P. and Ryu, J., 'Closed-form forward dynamic equations of 6 DOF PUS type parallel manipulators', *Proc. ASME Design Engineering Technical Conferences* (DETC2000), Baltimore, MD, 2000.

15. Kim, J. P. and Ryu, J., 'Inverse Kinematic and Dynamic Analysis of 6 DOF PUS type parallel manipulators', *Proc. Int. Workshop on Parallel Kinematic Machine* (PKM2000), 2000, 274–283.

16. Schiehlen, W., *Multibody Systems Handbook*, Springer-Verlag: New York, 1990.

17. Blajer, W., Schiehlen, W. and Schirm, W., 'Dynamic analysis of constrained multibody systems using inverse kinematics', *Mechanism and Machine Theory*, **28**(3), 1993, 397–405.

18. Angeles J. and Lee, S., 'The formulation of dynamical equations of holonomic mechanical systems using a natural orthogonal complement', *ASME J. of Applied Mechanics*, **55**, 1988, 243–244.

19. Angeles J. and Ma, O., 'Dynamic simulation of n-axis serial robotic manipulators using a natural orthogonal complement', *Int. J. of Robotics Res.*, **7**(5), 1988, 32–47.

20. Saha, S. K. and Angeles, J., 'Dynamics of nonholonomic mechanical systems using a natural orthogonal complement', *ASME Trans. J. of Applied Mechanics*, **58**, 1991, 238–243.

21. Ma, O. and Angeles, J., 'Performance evaluation of path-generating planar, spherical and spatial four-bar linkages', *Mechanism and Machine Theory*, **23**(4), 1988, 257–268.

22. Ma, O., *Mechanical analysis of parallel manipulators with simulation, design and control applications*, Ph.D. Thesis, Dept. of Mechanical Eng., McGill University, Montreal, Canada, 1991.

23. Xi, F. and Sinatra, R., 'Inverse dynamics of hexapods using the Natural Orthogonal Complement method', *J. of Manufacturing Systems*, **21**(2), 2002, 73–82.

24. Saha, S. K., 'Dynamics of Serial Multibody Systems using the Decoupled Natural Orthogonal Complement Matrices', *ASME J. of Applied Mech.*, **66**, 1999, 986–996.

25. Saha, S. K. and Schiehlen, W. O., 'Recursive Kinematics and Dynamics for Parallel Structured Closed-loop Multibody Systems', *Mech. Struct. Mach.*, **29**(2), 2001, 143–175.

26. Khan, W. A., *Distributed dynamics of systems with closed kinematic chains*, M. Eng. Thesis, Dept. Mechanical Eng., McGill University, Montreal, Canada, 2002.

27. Bonev, I. A. and Ryu, J., 'A geometrical method for computing the constant-orientation workspace of 6-*PRRS* parallel manipulators', *Mechanism and Machine Theory*, **36**(1), 2001, 1–13.

28. Stewart, G. W., *Introduction to matrix computations*, Academic Press, Inc., London, 1973.